Food Additives and Contaminants
Vol. 27, No. 5, May 2010, 701–709

Taylor & Francis
Taylor & Francis Group

Correlation and classification of single kernel fluorescence hyperspectral data with aflatoxin concentration in corn kernels inoculated with *Aspergillus flavus* spores

H. Yao[a]*, Z. Hruska[a], R. Kincaid[a], R. Brown[b], T. Cleveland[b] and D. Bhatnagar[b]

[a]*Geosystems Research Institute/Mississippi State University, Building 1103, Suite 118, Stennis Space Center, MS 39529, USA;* [b]*Southern Regional Research Center, Agricultural Research Service, United States Department of Agriculture, 1100 Robert E. Lee Boulevard, New Orleans, LA 70124, USA*

(*Received 14 October 2009; final version received 3 December 2009*)

The objective of this study was to examine the relationship between fluorescence emissions of corn kernels inoculated with *Aspergillus flavus* and aflatoxin contamination levels within the kernels. Aflatoxin contamination in corn has been a long-standing problem plaguing the grain industry with potentially devastating consequences to corn growers. In this study, aflatoxin-contaminated corn kernels were produced through artificial inoculation of corn ears in the field with toxigenic *A. flavus* spores. The kernel fluorescence emission data were taken with a fluorescence hyperspectral imaging system when corn kernels were excited with ultraviolet light. Raw fluorescence image data were preprocessed and regions of interest in each image were created for all kernels. The regions of interest were used to extract spectral signatures and statistical information. The aflatoxin contamination level of single corn kernels was then chemically measured using affinity column chromatography. A fluorescence peak shift phenomenon was noted among different groups of kernels with different aflatoxin contamination levels. The fluorescence peak shift was found to move more toward the longer wavelength in the blue region for the highly contaminated kernels and toward the shorter wavelengths for the clean kernels. Highly contaminated kernels were also found to have a lower fluorescence peak magnitude compared with the less contaminated kernels. It was also noted that a general negative correlation exists between measured aflatoxin and the fluorescence image bands in the blue and green regions. The correlation coefficients of determination, r^2, was 0.72 for the multiple linear regression model. The multivariate analysis of variance found that the fluorescence means of four aflatoxin groups, <1, 1–20, 20–100, and $\geq$100 ng g^{-1} (parts per billion), were significantly different from each other at the 0.01 level of alpha. Classification accuracy under a two-class schema ranged from 0.84 to 0.91 when a threshold of either 20 or 100 ng g^{-1} was used. Overall, the results indicate that fluorescence hyperspectral imaging may be applicable in estimating aflatoxin content in individual corn kernels.

Keywords: analysis – near infrared (NIR); regression; mycotoxins – aflatoxins; cereals and grain

Introduction

Certain organic and inorganic substances exhibit natural, intrinsic fluorescence when excited under an ultraviolet (UV) light source. Under UV excitation, plants can emit a fluorescence spectrum ranging from about 400 to 800 nm. In plant monitoring, for example, UV-induced fluorescence has been considered for various applications, including species identification and the detection of physiological disorders, pathogen attacks, and nutrient stresses (Dahn et al. 1992). The potential of UV-induced fluorescence of green plants for corn-weed discrimination has also been evaluated (Longchamps et al. 2009).

Aflatoxin-contaminated corn kernels also exhibit fluorescence under UV excitation. Aflatoxin is a naturally occurring secondary metabolite of *Aspergillus flavus*, and other fungi, in infected corn kernels when a corn plant is under heat and drought stress in the early dough stage. Contamination of corn with aflatoxins causes financial losses for growers and is a potential health hazard to animals and humans. The US Food and Drug Administration (USFDA) has established restrictions for aflatoxin levels present in food or feed. These levels (US Department of Agriculture (USDA) 2002) allow farmers, the food industry, and the Federal Grain Inspection Service (FGIS) to take appropriate actions when aflatoxin is found in food or feed.

It was reported that aflatoxin emits fluorescence when excited with UV light (Carnaghan et al. 1963; Goryacheva et al. 2008). In addition, *A. flavus*-infected grains also emit bright greenish yellow fluorescence (BGYF) under UV excitation. The relationship between *A. flavus* infection, BGYF, and aflatoxin was reported in a study with cotton seed (Marsh et al. 1969). It was pointed out that the ability of emitting

*Corresponding author. Email: haibo@gri.msstate.edu

ISSN 0265–203X print/ISSN 1464–5122 online

DOI: 10.1080/19440040903527368
http://www.informaworld.com

fluorescence is a characteristic of living cells that exhibit peroxidase activity. In the case of *A. flavus*, the fungus must infect the plant tissue and grow in it for some time, producing and transforming kojic acid, another known *A. flavus* metabolite, to one or more BGYF compounds in a peroxidase-type reaction. Furthermore, Lee et al. (1986) indicated that kojic acid, the BGYF compound, and aflatoxins are all formed during secondary metabolism.

Because of the apparent overlap between BGYF compound as well as aflatoxin production, the BGYF phenomenon has been widely used in presumptive tests for the presence of aflatoxin in corn (Bothast and Hesseltine 1975; Shotwell and Hesseltine 1981; Maupin et al. 2003) and other agricultural products such as pistachio nuts (Hadavi 2005) in order to determine if chemical analysis is required to measure the level of aflatoxin concentration. This approach has been used in inspection of whole-kernel corn or a stream of coarsely ground corn meal under 365 nm UV light, sometimes referred to as black light (Shotwell and Hesseltine 1981).

This approach, however, encounters both false-positive and false-negative detection. False-positive samples are healthy samples falsely regarded as being contaminated (Bothast and Hesseltine 1975), and false-negative detection is when contaminated samples are regarded as healthy samples, even when high aflatoxin contamination was found in non-BGYF corn (Widiastuti et al. 1988). The reason why black light inspection of BGYF is not a reliable test for aflatoxin-contaminated corn was explained by Wicklow (1999). Based on the literature, fluorescence is emitted from both aflatoxin and the BGYF compound, whether it is from toxin or non-toxin-producing *A. flavus*, all intermixed. This in turn produces high rates of false detection because the black light-based visual inspection cannot differentiate the fluorescence signals. The black light basically reveals the broad fluorescence response from the samples. However, it cannot identify the source of fluorescence emission. For this reason, the BGYF approach is only used as a presumptive test rather than quantitative or even qualitative analysis.

Thus, it would be helpful in aflatoxin detection if narrow band fluorescence was used in the process. In an early study on toxicity and fluorescence properties of aflatoxins, it was reported that different aflatoxin components gave different emission peaks (Carnaghan et al. 1963). The experiment measured fluorescence response of aflatoxin in methanol solution excited with 365 nm UV light. The emission peak wavelengths were 425, 425, 450, and 450 nm for aflatoxin B1, B2, G1, and G2, respectively. Carlson et al. (1999) used a fluorometer for aflatoxin detection. Their paper claimed that pure aflatoxin under a 365 nm excitation source will emit fluorescence at 445 nm.

Early research explored the fluorescence characteristics of aflatoxin for aflatoxin detection in agricultural products. Birth and Johnson (1970) measured the fluorescence response of single moldy corn kernels with a 365-nm UV excitation source. This study used a monochromator coupled with a $x-y$ recorder to log fluorescence energy versus wavelength. It was found that the logarithmic difference of fluorescence at 442 and 607 nm gave the best results for determining mould-contaminated corn kernels. However, there was no toxin measurement involved in the experiment.

Tyson and Clark (1974) investigated the fluorescence properties of single aflatoxin-infected pecans excited at 365 nm. The results concluded that fluorescence magnitude ratios can be used for aflatoxin detection. Of the two treatments, including soaking with aflatoxin and inoculation with *A. flavus* in the study, two fluorescence ratios were generated, 440/490 and 450/490 nm. The corresponding correlations between aflatoxin and the two ratios were 0.855 and 0.829. Further studies (Farsaie et al. 1978; McClure and Farsaie 1980) proposed the use of a fluorescence ratio of 490/420 nm for sorting aflatoxin-contaminated pistachio nuts. The excitation wavelength of the source was at 360 nm. These studies utilized visual inspection instead of chemical analysis for the separation of contaminated nuts. Farsaie et al. (1981) also suggested the use of a 420 nm excitation source for pistachio sorting.

Due to technological limitations, these previous experiments had many drawbacks. For example, the analogue spectrophotometers used in the study for fluorescence measurement had a coarse spectral resolution which made it difficult to differentiate subtle fluorescence changes. The fluorescence data also lacked spatial resolution when data were collected from a portion of a single kernel. Also, most studies did not provide chemical analysis for proper algorithm training and validation purposes, which render the results questionable.

In the past decade, fluorescence hyperspectral imaging technology has been developed to enable the acquisition of fluorescence image data with both high spectral and spatial resolutions (Kim et al. 2001; Zavattini et al. 2004) and was utilized when studying corn contaminated with aflatoxin (Yao et al. 2006). A fluorescence hyperspectral imaging system is generally based on an imaging spectrometer or hyperspectral imager. A single hyperspectral image has a spectral resolution between 1 nm and several nanometers, with the number of bands ranging from tens to hundreds. High spectral resolution images can be used to study the physical characteristics of an object at the pixel level by looking at the shape of the spectral reflectance.

The objective of the present study was to determine the relationship between fluorescence emission of corn kernels inoculated with *A. flavus* and aflatoxin contamination levels within the corn. The kernel

fluorescence emission data were measured with a fluorescence hyperspectral imaging system when corn kernel was excited with 365 nm UV light. The aflatoxin contamination level of the imaged single corn kernels was subsequently chemically measured using affinity column chromatography.

Materials and methods

Sample preparation

Corn plants were cultivated and harvested in Tifton, Georgia, where each ear of corn was inoculated at an early dough stage, with a toxigenic strain of *A. flavus* in order to induce aflatoxin infection. The aflatoxin-producing strain, AF13, was obtained from the USDA Southern Regional Research Center located in New Orleans, Louisiana. The *A. flavus* strain was seeded on potato dextrose agar in plastic Petri dishes under sterile conditions and incubated in the dark at 30°C for 7 days before being collected and diluted with sterile distilled water. A haemocytometer was used to determine the concentration of spores, and the solution was adjusted with sterile water until a dilution of 4×10^6 spores ml^{-1} was achieved. This culture stock was then used to inoculate the ears of corn in the field. The field inoculation was accomplished by injecting 3.0 ml of inoculum into the side of each ear. With this technique, a 12-gauge stainless steel needle was inserted into the side of each ear and the inoculum was injected into the ear through the husk.

After harvest, the inoculated ears were dried in a large forced air drier. The dry husks were removed under a chemical hood in order to limit exposure to potentially harmful dust particles and cross-contamination. All ears were examined under a 365 nm UV light source to identify any kernels exhibiting fluorescence. All kernels exhibiting fluorescence were carefully extracted using a small stainless steel laboratory spatula. In addition, kernels adjacent to the fluorescing kernels were also extracted to assess the spread of inoculum. Several kernels located away from the fluorescing kernels that did not exhibit fluorescence were used as controls (Figure 1). The side needle inoculation technique often damaged the individual kernels that were pierced by the needle; therefore, an effort was made to select only whole, undamaged kernels for imaging. The total sample comprised of 504 individual kernels.

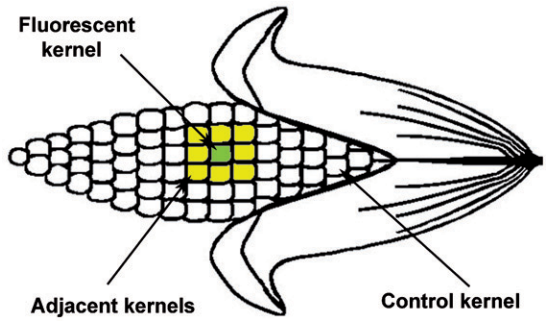

Figure 1. Corn kernel sample selection on an *A. flavus*-inoculated ear.

Fluorescence hyperspectral imaging

A fluorescence hyperspectral imaging system developed at Institute for Technology Development (ITD, Stennis Space Center, MS, USA) was used for this study. The fluorescence hyperspectral imaging system includes the VNIR 100E hyperspectral imaging system from ITD and a fluorescence excitation light source. The VNIR 100E integrated a patented line scanning technique (Mao 2000) using a push-broom line scanning system that requires no relative movement between the target and the sensor. The hyperspectral camera was a 14-bit PCO1600 CCD (charge-coupled device) high-resolution camera from the Cooke Corporation (Romulus, MI, USA). The fluorescence excitation light source used was a long wave (UV-A) ultraviolet lamp assembly (Model XX-15A) from Fisher Scientific (Thermo Fisher Scientific, Inc., Waltham, MA, USA) with wavelength centred at 365 nm and a power output of 196 MW.

For imaging set-up, the bottom of the camera lens was 22.2 cm above the target. The distance from the UV light to the target was 29.2 cm. At this distance, the light intensity was 605 $\mu w\,cm^{-2}\,nm^{-1}$. The light intensity was measured using an AvaSpec-ULS2048-USB2 spectrometer (Avantes BV, Eerbeek, The Netherlands) calibrated for irradiance measurement with a 10 ms integration time. Both the camera and the light were mounted together facing down toward the target.

Images were acquired under stable conditions in a dark imaging laboratory. No external light entered the imaging laboratory, and every effort was made to eliminate stray light emitted by the instruments used in the imaging process. The target was a rectangular ceramic plate containing both the contaminated and the control corn kernels. The plate was painted with flat, non-reflective black paint to reduce the amount of reflected light reaching the sensor. The colour of the plate also helped greatly to enhance the contrast between the background and the individual kernels. There was a grid of small, circular depressions on the upper surface of the plate designed to hold a single kernel. These depressions helped stabilize the kernels so that did not change position between image acquisitions. When placed on the plate, the kernels were not in contact with one another and could be individually segmented out in later image processing. A dark current image was also taken with the lens cap on and all lights off for calibration purposes.

Chemical analysis for sample reference

After imaging, the corn kernel samples were chemically analysed for aflatoxin content to obtain correlating measurements using the following procedure adapted from the protocol obtained from VICAM (Milford, MA, USA). The VICAM AflaTest is one of the aflatoxin-determination laboratory methods approved by USDA. Briefly, each dry corn kernel was first crushed and weighed in a pre-labelled glass vial. In order to simplify the procedure, a uniform sample of 100 mg was used for aflatoxin extraction. Samples were extracted with methanol/water (80/20%). A total of 2 ml of methanol/water was added to each 100 mg sample and placed on a shaker for 30 min. A total of 1 ml of each extract was diluted 1 : 4 with distilled water and filtered twice before passage through the AflaTest affinity columns. The first filtration was through a coarse fluted filter, and the second through a glass filter. The columns were washed twice with 5 ml distilled water and eluted with 1 ml of pure methanol. A total of 1 ml of developer, provided in the AflaTest kit, was added to each eluted sample. Each sample was vortexed and aflatoxin concentration in parts per billion ($ng\,g^{-1}$) was measured with the Series 4EX Fluorometer (VICAM). The resulting 0.2 g equivalent was multiplied by five to obtain a 1 g equivalent aflatoxin content of each sample.

Image processing

Each raw hyperspectral image was preprocessed using several steps. First, image sensor background noise was removed through dark current subtraction using dark current data previously collected. Next, each image band was assigned with its appropriate wavelength. Because the sample fluorescence response was distributed mainly over the 400–600 nm range, and the image contained relatively high levels of background noise in the range 900–1000 nm, the original image bands were spectrally subset to retain only the relevant data from 399.68 to 601.36 nm for a total of 74 bands. The last step was the random noise removal. In this step, a low-pass spectral filter was used to run moving averages along the wavelength for each pixel. The low-pass filter had a window size of five bands. After preprocessing, the image had 74 bands with a wavelength range of 400–600 nm. The resulting image of 800×425 pixels had an image size of 98 Mbytes.

From each preprocessed plate image, the whole-kernel reflectance of each corn kernel had to be extracted for statistical analysis. For this step, an image spectral threshold process was used to build a mask image with corn kernels in the foreground and the plate in the background (Figure 2). The threshold process used one image band of the fluorescence hyperspectral image. The mask image was applied to the corresponding hyperspectral image to create a region of interest (ROI) for each corn kernel. The whole kernel spectral fluorescence was averaged and extracted over the whole kernel ROI.

Statistical analysis

After the previous processing steps, the resulting data of each corn kernel consisted of one aflatoxin concentration measurement and 74 average fluorescence spectral readings for a total of 504 kernels. The subsequent statistical analysis included several multivariate statistical procedures. The multiple linear regression, multivariate analysis of variance, and discriminant analysis were implemented with the SAS® program. For data illustration, aflatoxin data distribution, correlation coefficients between each image band and aflatoxin measurements, and the mean fluorescence spectra for different aflatoxin concentration levels are also presented in the Results section. The multivariate analysis of variance used four aflatoxin levels in $ng\,g^{-1}$ (ppb). The four levels are <1, 1–20, 20–100, and $>100\,ng\,g^{-1}$. These levels were

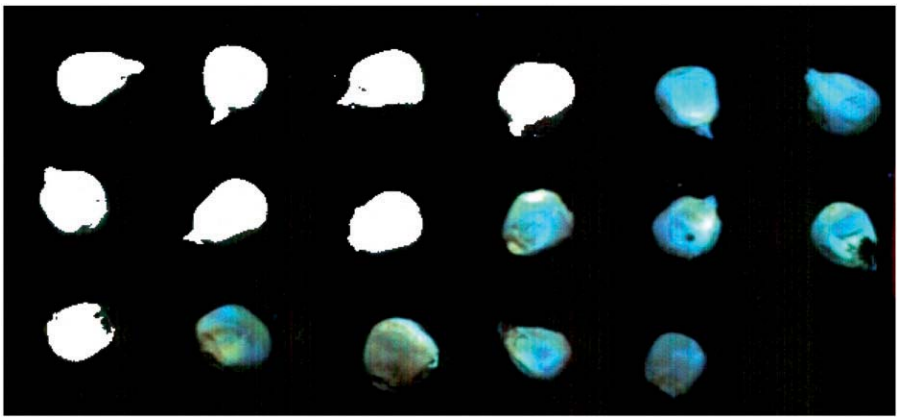

Figure 2. Illustration of corn kernel samples for imaging and image threshold-processing for fluorescence spectral extraction.

developed based on pre-existing USFDA regulations against sale of aflatoxin-contaminated commodities (USDA 2002). Generally, 20 ng g^{-1} and lower is considered safe for human food consumption or dairy feed (because the potential carryover of AFM1 to the milk), and 100 ng g^{-1} and lower is safe for animal feed. Any sample containing greater than 100 ng g^{-1} of aflatoxin must be destroyed. One exception is the feed for finishing cattle where the acceptable levels are up to 300 ng g^{-1}.

Results and discussion

Corn kernel distribution based on visual inspection using 365 nm UV light and aflatoxin levels through VICAM chemical analysis is presented in Table 1. Of the total 504 single corn kernels, 180 kernels (35.7%) were found to have aflatoxin levels <1 ng g^{-1}, 130 kernels (25.8%) between 1 and 20 ng g^{-1}, 31 kernels (6.2%) between 20 and 100 ng g^{-1}, and 163 (32.3%) >100 ng g^{-1}.

Figure 3 represents the mean fluorescence spectra for the different groups of corn kernels with different aflatoxin contamination levels. Corn fluorescence emission was found mainly to distribute in the blue and green spectral regions. The peak emissions were all in the blue region with peak locations below 500 nm. The shapes of the fluorescence spectral curves were similar for different contamination groups. However, there existed distinct differences among the groups both in fluorescence magnitudes and fluorescence peak locations. Generally, less contaminated corn kernels exhibited higher fluorescence response. The most contaminated corn kernels (≥100 ng g^{-1}) had the lowest fluorescence response. Another distinct feature among the curves was the existence of a fluorescence peak shift (FPS). From Figure 3 it is evident that the FPS for low- or non-contaminated corn is toward the short wavelength of the spectrum. The FPS for medium- or highly contaminated corn is toward the long wavelength of the spectrum. For example, corn kernels with <1 or 1–20 ng g^{-1} aflatoxin contamination have fluorescence peaks located around 465 nm. The peak also shifts toward longer wavelength when contamination level increases. The 20–100 ng g^{-1} group has a peak at around 475 nm and the ≥100 ng g^{-1} group has a peak

Table 1. Distribution of aflatoxin levels in corn samples.

	Aflatoxin distribution in corn kernel samples (%)				
Visual inspection	<1 ng g^{-1}	1–20 ng g^{-1}	20–100 ng g^{-1}	≥100 ng g^{-1}	Total number
BGYF	19.18	9.13	4.57	67.12	219
Non-BGYF	48.42	38.60	7.37	5.61	285

Note: BGYF, bright greenish yellow fluorescence.

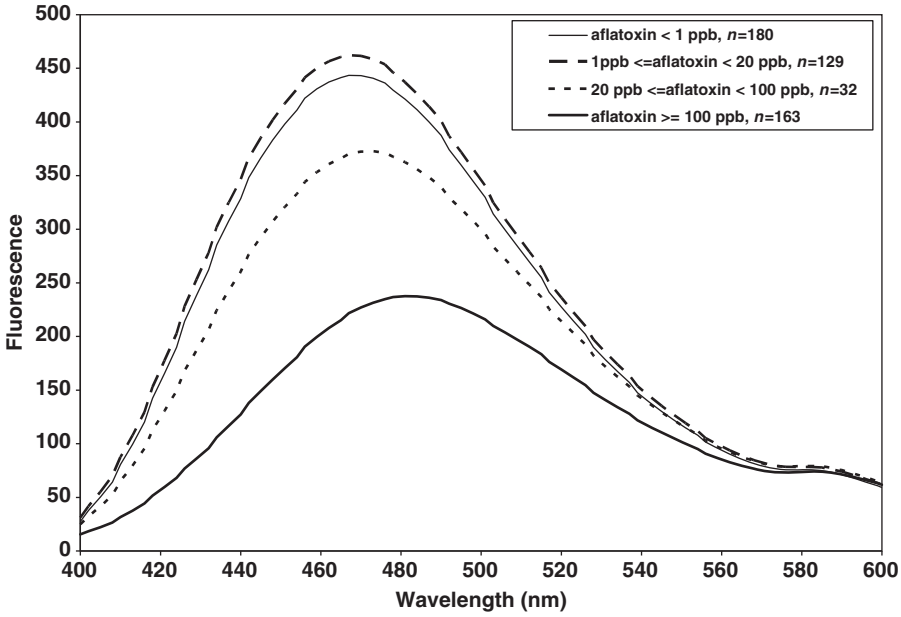

Figure 3. Mean fluorescence spectra of corn kernels with different contamination levels.

around 485 nm. The bandwise correlations between each fluorescence band and corresponding aflatoxin measurement are presented in Figure 4. Correlations were calculated between aflatoxin content of each corn kernel and fluorescence emission spectrum across all wavelengths in the 400–600 nm range. Except for a weak positive correlation at around 600 nm, a negative correlation of the two measures was observed throughout the fluorescence region. The highest correlation was noted between 400 and 450 nm with $r = -0.67$.

The present observation indicates that both fluorescence peak magnitude and FPS are suitable parameters for *in-situ* detection and estimation of the levels of aflatoxin contamination in corn.

Multiple linear regression

The scatter plot shown in Figure 5 demonstrates the predicted aflatoxin versus actual aflatoxin (all in ng g^{-1}) in single corn kernels. The aflatoxin prediction model used multiple linear regression (SAS 2007) with all 74 fluorescence bands. The original model resulted in a coefficient of determination, $r^2 = 0.67$. Since the original model makes a negative estimation of aflatoxin levels, the adjusted model on the right side of Figure 5 forces negative prediction of aflatoxin into zero. The adjusted model thus has an $r^2 = 0.72$. Overall, this model indicates that there exists a modest correlation between the predicted and actual aflatoxin levels in the corn kernels.

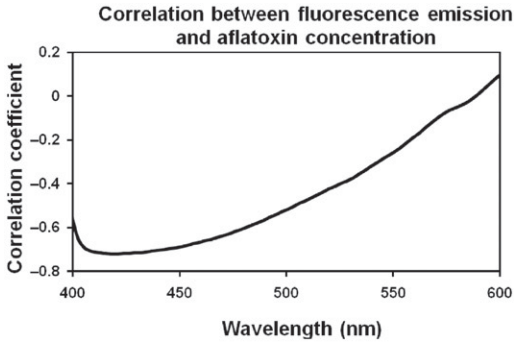

Figure 4. The fluorescence emission of each kernel measured by the VNIR sensor was correlated with aflatoxin concentrations across all wavelengths. The highest correlation of the two measures was centred between 400 and 450 nm where the correlation coefficient was $r = -0.67$.

Multivariate analysis of variance

Multivariate analysis of variance (MANOVA) was employed in order to determine whether fluorescence hyperspectral spectra could be used to separate the four groups of aflatoxin data. MANOVA is a statistical procedure generally used to test for significant group differences. More specifically, MANOVA tests for differences among the multivariate centroids of groups. Thus, the question required testing the hypothesis that there was no difference in the fluorescence spectra among the four aflatoxin levels. MANOVA also takes into consideration the relationship between independent and dependent variables (SAS 2007). Table 2 displays results for the equal mean test from MANOVA. The four test criteria all had $p < 0.0001$, which indicates, when $\alpha = 0.01$, that the multivariate effect of aflatoxin level is statistically significant. In other words, the mean fluorescence spectra of the four groups were significantly different from each other. Table 3 summarizes the MANOVA test for equal means for pairwise comparison between all groups. The results show that a *p*-value between the

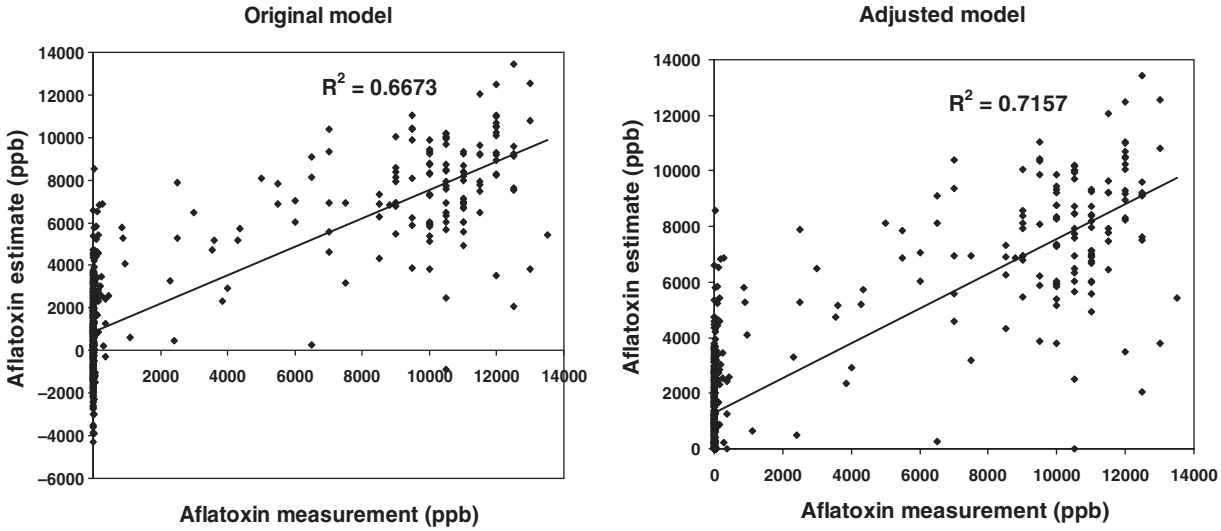

Figure 5. Multiple regression model of aflatoxin concentration using fluorescence hyperspectral information of corn. The scatter plot shows estimated aflatoxin versus actual aflatoxin (all in ng g^{-1}) in single corn kernels. The aflatoxin prediction model used multiple linear regression with all 74 fluorescence bands.

<1 and 1–20 ng g^{-1} group is 0.02, indicating that means for the two groups are not significantly different when $\alpha = 0.01$. For the rest of the comparisons, each pair of means is significantly different from each other when $\alpha = 0.01$.

Discriminant analysis

For discriminant analysis, the problem was treated as a two-class problem. The analysis classified each sample into one of the two classes for a given threshold, whether the sample belonged to a class below the threshold (control) or above (contaminated). The threshold levels used were 20 and 100 ng g^{-1}. When running the discriminant analysis in SAS, two discriminant analysis models, re-substitution and cross-validation, were used to estimate the error (misclassification rate) of a classifier. Re-substitution constructs a single classifier based on all the data. Each data observation is then passed through the classifier to decide if the single data observation can be correctly classified. Classification result is summarized after all data are examined by the classifier. Cross-validation (in leave-one-out form) removes each observation in turn, constructs the classifier, and then computes whether this leave-one-out classifier correctly classifies the deleted observation. All 74 bands from the data were used in the analysis. The analysis results are presented in Table 4, including average classification accuracies. The classification accuracy is generally in the upper 80s or lower 90s. Overall, the resubstitution model shows higher classification accuracy compared with the cross-validation model. The two models differ in classifier error estimates.

Conclusions

In the present study, fluorescence emission spectra of aflatoxin-contaminated corn kernels were collected with a VNIR hyperspectral imaging system in order to investigate the relationship between aflatoxin levels and fluorescence emission peaks. Past studies suggested that fluorescence emission from aflatoxin-contaminated corn kernels could be a mixed fluorescence response from both aflatoxin and the BGYF compound formed from kojic acid. In the current experiment, fluorescence hyperspectral images were collected from single kernels excited with 365 nm UV light. The corn kernels were extracted from corn ears

Table 4. Two-class discriminate analysis using fluorescence hyperspectral data (74 bands in the range 400–600 nm). The ng g^{-1} level was used to determine the two classes: contaminated (≥ng g^{-1} level) and control (<ng g^{-1} level).

		Average classification accuracy (%)	
	ng g^{-1} (ppb)	20	100
Classification Method	Resubstitution	87	91
	Cross-validation	84	86

Table 2. The General Linear Models (GLM) Procedure: results of the multivariate analysis of variance (MANOVA) test for equal mean hypothesis for all four aflatoxin levels for the hypothesis of no overall level effect.

Statistic	Value	*F*-value	Num DF	Den DF	$Pr > F$
Wilks' Lambda	0.21612056	3.85	222	1281.4	<0.0001
Pillai's Trace	1.04273166	3.09	222	1287	<0.0001
Hotelling–Lawley Trace	2.53043404	4.85	222	1213.5	<0.0001
Roy's Greatest Root	2.07393306	12.02	74	429	<0.0001

Note: Num DF, the number of degrees of freedom in the model; Den DF, the number of degrees of freedom associated with the model errors.

Table 3. Results of the multivariate analysis of variance (MANOVA) test for equal means for pairwise comparisons between all groups.

	Pairwise comparison between groups			
p-value	<1 ng g^{-1}	1–20 ng g^{-1}	20–100 ng g^{-1}	≥100 ng g^{-1}
<1 ng g^{-1}	n.a.	0.0196	0.0024	<0.0001
1–20 ng g^{-1}	0.0196	n.a.	0.0091	<0.0001
20–100 ng g^{-1}	0.0024	0.0091	n.a.	<0.0001
≥100 ng g^{-1}	<0.0001	<0.0001	<0.0001	n.a.

Note: n.a., Not available.

artificially inoculated with aflatoxin-producing *A. flavus*. Each corn kernel was then chemically analysed to determine the aflatoxin contamination levels using fluorometry. A fluorescence peak shift phenomenon was discovered among different groups of kernels with different aflatoxin contamination levels. The FPS moved toward a longer wavelength in the blue region for the highly contaminated kernels and toward a shorter wavelengths for clean or less contaminated kernels. Highly contaminated kernels also had a lower fluorescence peak magnitude compared with less contaminated kernels. A general negative correlation was also discovered between measured aflatoxin and the fluorescence image bands in the blue and green spectral regions. The adjusted multiple linear regression model resulted in an $r^2 = 0.72$ indicating a modest correlation between the predicted and actual aflatoxin levels in the corn kernels. The multivariate analysis of variance results indicated that the fluorescence emission means of the four aflatoxin groups: <1, 1–20, 20–100, and $\geq 100\,\mathrm{ng\,g^{-1}}$, are significantly different at $\alpha = 0.01$. Finally, discriminant analysis found that when corn samples were classified into two classes using a threshold of either 20 or $100\,\mathrm{ng\,g^{-1}}$, the classification accuracy ranged from 0.84 to 0.91 based on different ways of error evaluation.

Overall, the results clearly illustrate the potential of using fluorescence hyperspectral imaging methodology for estimating aflatoxin content in individual corn kernels. The unique fluorescence peak feature in contaminated corn kernels revealed by the method in the present study may be further explored by applying the method to toxigenic and atoxigenic strains of *A. flavus*. In addition, the influence of germ and endosperm sides of the corn kernels on the FPS would also be of interest. Results from these experiments could provide valuable information for developing new aflatoxin detection and estimation technologies for the corn industry.

Acknowledgements

Funding for this work was provided by the US Department of Agriculture (USDA) (Cooperative Agreement Number 58-6435-3-121). The authors would like to thank Dr Matthew Krakowsky from the USDA/ARS, Tifton, Georgia, for help with producing the corn samples for this study, including planting, inoculation, and harvesting.

References

Birth GS, Johnson RM. 1970. Detection of mold contamination in corn by optical measurements. J Assoc Off Anal Chem. 53:931–936.

Bothast RJ, Hesseltine CW. 1975. Bright greenish-yellow fluorescence and aflatoxin in agricultural commodities. Appl Microbiol. 30:337–338.

Carlson MA, Bargeron CB, Benson RC, Fraser AB, Goopman JD, Ko HW, Philips TE, Strickland PT, Velky JT. 1999. Development of an automated handheld immunoaffinity fluorometris biosensor. Johns Hopkins APL Technical Digest. 20:372–380.

Carnaghan RB, Hartley RD, O'Kelly J. 1963. Toxicity and fluorescence properties of the aflatoxins (*Aspergillus flavus*). Nature. 14(200):1101–1101.

Dahn HG, Gunther KP, Ludecker W. 1992. Characterisation of drought stress of maize and wheat canopies by means of spectral resolved laser induced fluorescence. EARSeL Adv Remote Sensing. 1:12–19.

Farsaie A, McClure WF, Monroe RJ. 1978. Development of indices for sorting Iranian pistachio nuts according to fluorescence. J Food Sci. 43:1550–1552.

Farsaie A, McClure WF, Monroe RJ. 1981. Design and development of an automatic electro-optical sorter for removing BGY fluorescent pistachio nuts. Trans ASAE. 24:1372–1375.

Goryacheva IY, Rusanova TY, Pankin KE. 2008. Fluorescent properties of aflatoxins in organized media based on surfactants, cyclodextrins, and calixresorcinarenes. J Anal Chem. 63:751–755.

Hadavi E. 2005. Several physical properties of aflatoxin-contaminated pistachio nuts: application of BGY fluorescence for separation of aflatoxin-contaminated nuts. Food Addit Contamin. 22:1144–1153.

Kim MS, Chen YR, Mehl PM. 2001. Hyperspectral reflectance and fluorescence imaging system for food quality and safety. Trans ASAE. 44:721–729.

Lee LS, Parrish FW, Jacks TJ. 1986. Substrate depletion during formation of aflatoxin and kojic acid on corn inoculated with *Aspergillus flavus*. Mycopathologia. 93:105–107.

Longchamps L, Panneton B, Samson G, Leroux GD, Theriault R. 2009. Discrimination of corn, grasses and dicot weeds by their UV-induced fluorescence spectral signature. Precision Agriculture. Published online 30 June. Available from: http://www.springerlink.com/content/h367920v08414804/.

Mao C. 2000. Focal plane scanner with reciprocating spatial window. US Patent 6,166,373.

Marsh PB, Simpson ME, Ferretti RJ, Merola GV, Donoso J, Craig GO, Trucksess MV, Work PS. 1969. Mechanism of formation of a fluorescence in cotton fiber associated with aflatoxin in the seeds at harvest. J Agricult Food Chem. 17:468–472.

Maupin LM, Clements MJ, White DG. 2003. Evaluation of the MI82 Corn Line as a source of resistance to aflatoxin in grain and use of BGYF as a selection tool. Plant Dis. 87:1059–1066.

McClure WF, Farsaie A. 1980. Dual-wavelength fiber optic photometer measures flourescence of aflatoxin-contaminated pistachio nuts. Trans ASAE. 23:204–207.

SAS. 2007. Multivariate statistical methods: Practical research applications. Cary (NC): SAS Institute, Inc.

Shotwell OL, Hesseltine CW. 1981. Use of bright greenish yellow fluorescence as a presumptive test for aflatoxin in corn. Cereal Chem. 58:124–127.

Tyson TW, Clark RL. 1974. An investigation of the fluorescent properties of aflatoxin-infected pecans. Trans ASAE. 17:942–944, 948.

US Department of Agriculture (USDA). 2002. Aflatoxin handbook. Washington (DC): USDA Grain Inspection Service Publication.

Wicklow DT. 1999. Influence of *Aspergillus flavus* strains on aflatoxin and bright greenish yellow fluorescence of corn kernels. Plant Dis. 83:1146–1148.

Widiastuti R, Maryam R, Blaney BJ, Salfina, Stoltz DR. 1988. Corn as a source of mycotoxins in Indonesian poultry feeds and the effectiveness of visual examination methods for detecting contamination. Mycopathologia. 102:45–49.

Yao H, Hruska Z, Brown RL, Cleveland TE. 2006. Hyperspectral bright greenish-yellow fluorescence (BGYF) imaging of aflatoxin-contaminated corn kernels. IN: Proceedings of SPIE, Optics for Natural Resources, Agriculture, and Foods. Vol. 6381, paper no. 63810B.

Zavattini G, Vecchi S, Leahy RM, Smith DJ, Cherry SR. 2004. A hyperspectral fluorescence imaging system for biological applications. 2003. IEEE Nuclear Science Symposium Conference Record. 2:942–946.